Vascular Permeability during Antiangiogenesis Treatment: MR Imaging Assay Results as Biomarker for Subsequent Tumor Growth in Rats[1]

Hans-Juergen Raatschen, MD
Gerhard H. Simon, MD
Yanjun Fu, PhD
Barbara Sennino, PhD
David M. Shames, MD
Michael F. Wendland, PhD
Donald M. McDonald, MD, PhD
Robert C. Brasch, MD

Purpose: To prospectively evaluate in rats the acute change in tumor vascular leakiness (K^{PS}) assayed at magnetic resonance (MR) imaging after a single dose of the angiogenesis inhibitor bevacizumab as a predictive biomarker of tumor growth response after a prolonged treatment course.

Materials and Methods: Institutional animal care and use committee approval was obtained. Seventeen female rats with implanted human breast cancers underwent dynamic albumin-$(Gd\text{-}DTPA)_{30}$–enhanced MR imaging followed by an initial dose of bevacizumab or saline (as a control). Treatment was continued every 3rd day, for a total of four doses at five possible dose levels: 0 mg bevacizumab ($n = 4$ [control rats]), 0.1 mg bevacizumab ($n = 3$), 0.25 mg bevacizumab ($n = 2$), 0.5 mg bevacizumab ($n = 5$), and 1.0 mg bevacizumab ($n = 3$). A second MR imaging examination was performed 24 hours after the initial dose to enable calculation of the acute change in MR imaging–assayed leakiness, or ΔK^{PS}. This acute change in K^{PS} at MR imaging was correlated with tumor growth response for each cancer at the completion of the 11-day treatment course. For statistical analyses, an unpaired two-tailed t test, analysis of variance, and linear regression analyses were used.

Results: The MR imaging–assayed change in tumor microvascular leakiness, tested as a potential biomarker, correlated strongly with tumor growth rate ($R^2 = 0.74$, $P < .001$). K^{PS} and tumor growth decreased significantly in all bevacizumab-treated cancers compared with these values in control group cancers ($P < .05$).

Conclusion: The MR imaging–assayed acute change in vascular leakiness after a single dose of bevacizumab was an early, measurable predictive biomarker of tumor angiogenesis treatment response.

[1] From the Department of Radiology, Center for Pharmaceutical and Molecular Imaging (H.J.R., G.H.S., Y.F., D.M.S., M.F.W., R.C.B.), Cardiovascular Research Institute, Comprehensive Cancer Center (B.S., D.M.M.), and Department of Anatomy, University of California San Francisco, San Francisco, Calif. From the 2006 RSNA Annual Meeting. Received February 21, 2007; revision requested May 8; revision received July 23; accepted August 17; final version accepted October 23. Supported in part by National Institutes of Health grants RO1 CA082923, HL-24136, and HL-59157. **Address correspondence to** H.J.R., Charite-Campus Benjamin Franklin, Department of Radiology, Hindenburgdamm 30, 12203 Berlin (e-mail: *hans-juergen.raatschen@charite.de*).

Primary goals for cancer biomarkers are to more reliably and accurately predict the risk of acquiring cancer and, once cancer is acquired, predict how a specific tumor will respond to a particular treatment. Diagnostic imaging and, more specifically, contrast material–enhanced magnetic resonance (MR) imaging, have the potential to be applied to obtain biomarkers of cancer treatment response.

Angiogenesis is essential for the growth and metastasis of most cancers and thus is a prime target for biomarker development (1–6). The upregulated formation of new blood vessels growing into a tumor from the surrounding noncancerous host tissues or some alternative mechanism of tumor vascularization is required if a cancer is to grow beyond a diameter of 2 mm (7,8).

Drug inhibitors of angiogenesis directly or indirectly alter the structure and function of microscopic tumor blood vessels, including their permeability to macromolecular solutes, in ways that can sometimes be detected and measured quantitatively with dynamic MR imaging (9–17). The dynamic contrast-enhanced MR imaging approach focuses directly on the tumor vessels and can be applied in such a manner as to take advantage of the vessels' well-documented macromolecular leakiness (18–21). The MR imaging assay of cancer microvascular permeability has been shown in experimental animal models (22–25) and more recently in human patients with breast cancer (26) to be a useful method for characterizing individual tumors. Results of past MR imaging studies with macromolecular contrast media have demonstrated the potential to differentiate benign from malignant lesions with a high probability (27), to noninvasively characterize tumors with positive correlations to histopathologic grade (27), and to monitor responses to antiangiogenic drug treatments (24,28), including a spectrum of drug classes: inhibitors of vascular endothelial growth factor (VEGF) (24,29), tyrosine kinase inhibitors of angiogenesis receptors (30), and matrix metalloproteinase inhibitors (31).

Prior to its clinical approval, bevacizumab (Avastin; Genentech, South San Francisco, Calif) was tested in MR imaging studies of athymic rats bearing human breast cancers and ovarian cancers and demonstrated a strong drug effect on microvascular macromolecular permeability; the MR imaging–assayed leakiness declined significantly and profoundly (>70%, $P < .01$) after either a 7-day course of therapy (32) or 24 hours after a single 1-mg dose of bevacizumab (17). Although MR imaging has been used to detect a decline in macromolecular microvessel leakiness as early as 24 hours after the initiation of antiangiogenic drug treatment (17), no attempt has been made to correlate this acute response with the effect of prolonged therapy.

We hypothesized that MR imaging of microvessel permeability to macromolecular contrast media can yield an early, noninvasive biomarker of tumor responsiveness to angiogenesis inhibition. Thus, the purpose of our study was to prospectively evaluate in rats the acute change in MR imaging–assayed tumor vascular leakiness (K^{PS}) after a single dose of the angiogenesis inhibitor bevacizumab as a predictive biomarker of tumor growth response after a prolonged treatment course.

Advance in Knowledge

- MR imaging–assayed tumor vascular leakiness measured 24 hours after a single dose of bevacizumab correlated strongly ($R^2 = 0.74$, $P < .001$) with the change in tumor growth measured after a prolonged multidose treatment course.

Implication for Patient Care

- Although not immediately applicable to patient care, our results may encourage the further development of MR imaging permeability assays and macromolecular contrast media to yield predictive biomarkers in cancer treatment monitoring.

Materials and Methods

Genentech provided the antiangiogenic drug bevacizumab. The authors maintained control of the data and information submitted for publication.

Animals and Experimental Protocol

The study was performed in accordance with the guidelines of the National Institutes of Health for the care and use of laboratory animals. Approval from the institutional Animal Care and Use Committee was obtained.

Five million MDA-MB-435 human breast cancer cells (ATCC, Manassas, Va) that represented poorly differentiated adenocarcinoma (33) and were suspended in a total volume of 0.5 mL of a 1:1 mixture of phosphate-buffered saline and Matrigel (BD Biosciences, Bedford, Mass) were injected subcutaneously into the right mammary fat pad of seventeen 4-week-old female homozygous athymic nude rats (Harlan, Indianapolis, Ind) (H.J.R., G.H.S., M.F.W.). Animals were visually checked every 2nd day for tumor size (H.J.R., G.H.S.). When tumors reached a diameter of 1.0–1.5 cm in largest dimension as measured with calipers, animals were randomly assigned to one of the treatment groups, each with a different dose of angiogenesis inhibitor. Then, a baseline dynamic MR imaging examination enhanced with a macromolecular

Published online before print
10.1148/radiol.2472070363

Radiology 2008; 247:391–399

Abbreviations:
Gd-DTPA = gadolinium diethylenetriaminepentaacetic acid
VEGF = vascular endothelial growth factor

Author contributions:
Guarantors of integrity of entire study, H.J.R., R.C.B.; study concepts/study design or data acquisition or data analysis/interpretation, all authors; manuscript drafting or manuscript revision for important intellectual content, all authors; manuscript final version approval, all authors; literature research, H.J.R., G.H.S., Y.F.; experimental studies, H.J.R., G.H.S., Y.F., B.S., M.F.W.; statistical analysis, H.J.R., D.M.S., M.F.W.; and manuscript editing, H.J.R., B.S., D.M.S., M.F.W., D.M.M., R.C.B.

See Materials and Methods for pertinent disclosures.

contrast medium, albumin-(gadolinium diethylenetriaminepentaacetic acid [Gd-DTPA])$_{30}$ (synthesized in our own lab), was performed (34) (H.J.R., G.H.S., M.F.W.). Albumin-(Gd-DTPA)$_{30}$ has a distribution volume that closely approximates the blood volume (0.05 L/kg) and a plasma half-life of approximately 120 minutes in rats. The contrast agent was injected in all 17 rats at a dose of 0.03 mmol gadolinium per kilogram of body weight. Immediately after MR imaging, treatment was initiated with bevacizumab, a humanized monoclonal antibody to VEGF, in one of five possible doses: 0 mg bevacizumab (n = 4 [control rats, which received saline]), 0.1 mg bevacizumab (n = 3), 0.25 mg bevacizumab (n = 2), 0.5 mg bevacizumab (n = 5), or 1.0 mg bevacizumab (n = 3); bevacizumab was given intraperitoneally in a total volume of 1.0 mL (H.J.R., G.H.S., Y.F., B.S.). The peritoneal route for bevacizumab administration is standard in rodents.

Bevacizumab has been shown to inhibit tumor angiogenesis and growth in vivo in different xenograft tumor models, is governmentally approved for the treatment of colon cancer (35), and is now being tested for additional human cancers (36).

The bevacizumab or saline treatment was continued with intraperitoneal injections every 3rd day, for a total of four doses spanning a total of 11 days. Twenty-four hours after the baseline MR imaging examination, a second MR imaging examination was performed in the same animals by using the same technique (H.J.R., G.H.S., M.F.W.). Tumor diameter was measured with calipers every 2nd day, from the initial day of treatment until 24 hours after the final dose of bevacizumab or saline (day 11). Tumor volumes were calculated in millimeters (H.J.R., G.H.S., Y.F.) according to the equation $L \cdot W \cdot H \cdot 0.52$, where L is length, W is width, and H is height; dimensions could be measured in all three planes because the tumor was situated and movable within the loose subcutaneous tissues. Tumor volume ratios were defined as the tumor volume on day x (V_x) divided by the tumor volume at baseline (V_0). Fractional tumor growth rates per day were determined with monoexponential fitting of the tumor volume values over time (H.J.R., D.M.S.).

MR Imaging and Data Analysis

For the MR imaging experiments, anesthesia was induced with intraperitoneal injection of 35 mg/kg sodium pentobarbital (Nembutal; Abbott Laboratories, North Chicago, Ill) and 0.025 mg/kg buprenorphine hydrochloride (Buprenex; Reckitt Benckiser Pharmaceuticals, Richmond, Va). A 25-gauge butterfly catheter (Abbott Laboratories) was inserted into a tail vein for contrast medium injection. Rats were placed on a heated deuterated-water pad to keep the body temperature at constant physiologic levels (H.J.R., G.H.S., Y.F.).

MR imaging was performed by using a system operating at 2.0 T (Omega CSI-II; Bruker Instruments, Fremont, Calif), in the range of commonly used clinical MR imaging units. This system is equipped with self-shielded gradient coils (Acustar S-150, 0.002 T/cm, 15-cm inner diameter). The rats were placed supine in a birdcage radiofrequency coil (inner diameter, 4.5 cm; length, 7.6 cm), enabling primary image acquisitions in the z-plane centered on the hemisphere of each tumor. A series of nine precontrast T1-weighted inversion-recovery centric-ordered fast gradient-echo sequences (repetition time msec/echo time msec, 6.0/1.5; number of signals acquired, one; flip angle, 10°; matrix, 64 × 64 × 16; field of view, 50 × 50 × 48; section thickness, 3 mm) with the inversion time varying between 100 and 2500 msec was performed to enable the calculation of baseline relaxation rates (R1) for each tumor. Each image was reconstructed in phase-sensitive mode, and R1 values for tumor regions were determined by performing a standard three-parameter fit of signal intensity (SI) data to the equation $SI = a - b \exp(-TI \cdot R1)$, as reported and described previously (29). Then, dynamic contrast-enhanced MR imaging was performed by using a transverse T1-weighted three-dimensional spoiled gradient-recalled acquisition in the steady state sequence that consisted of two precontrast and multiple dynamic postcontrast images obtained up to 1 hour after contrast material injection with the following parameters: 50/3; number of signals acquired, one; flip angle, 90°; matrix, 128 × 128 × 16; field of view, 50 × 50 × 48 mm; section thickness, 3 mm; number of sections acquired, 16; and acquisition time, 1 minute 42 seconds per image. The relatively long temporal resolution has been shown experimentally to be well suited to the relatively slow distribution kinetics of this molecularly large contrast medium.

Images were transferred to, processed with, and analyzed at a workstation (Sun Microsystems, Mountain View, Calif) by using commercially available image analysis software (MRVision; MRVision, Winchester, Mass). In each rat and at each time point, regions of interest were drawn over the blood in the inferior vena cava to cover the whole contrast-enhanced vessel lumen and over the tumor rim, as well as over the entire tumor, at the tumor equator (H.J.R., G.H.S.). The blood response measured in the inferior vena cava was used as an input function (37). Tumor rim was defined as the 2-mm zone around the tumor periphery, which has been shown previously to be relatively more sensitive to changes in angiogenesis than the whole tumor (38). Postcontrast R1 values ($R1_{post}$) were calculated on the basis of the measured signal intensity (SI) and the calculated precontrast R1 values ($R1_{pre}$) by using the equation $R1_{post} = -\ln\{1 - (SI_{post}/SI_{pre})[1 - \exp(-TR \cdot R1_{pre})]\}/TR$ (39), where SI_{post} is postcontrast signal intensity, SI_{pre} is precontrast signal intensity, and TR is repetition time in milliseconds. Precontrast R1 of blood was assumed to be 0.73 sec^{-1} on the basis of many historical measurements in other animals (39). Differences between the precontrast and postcontrast R1 values (ΔR1) at any time were taken to be proportional to the concentration of the contrast medium, either in the blood or in the tissue of interest.

The ΔR1 data from the blood and tumor were used for kinetic analysis involving the use of a two-compartment model to estimate the endothelial transfer coefficient (K^{PS}, in microliters per minute per cubic centimeter of tissue) (27) according to a two-compartment

tissue model (Fig 1). The endothelial transfer coefficient K^{PS} is a measure of leakiness of the contrast medium from the blood, or vascular compartment, into the extravascular extracellular compartment. A monoexponential function was found to provide good fits to the albumin-$(Gd\text{-}DTPA)_{30}$ blood ΔR1 data. Tumor ΔR1 data were fitted by using a two-compartment bidirectional kinetic model (40) (H.J.R., G.H.S., D.M.S.). The reflux rate constant of this model was not resolvable from the data and was therefore set to zero. All data fitting was performed by using software (SAAM II; SAAM Institute, Seattle, Wash) that employed a weighted nonlinear least-squares parameter estimation algorithm (41). Measurement errors in the ΔR1 data were assumed to be independent and Gaussian, with zero mean and fractional standard deviation known within a scale factor determined from the data. Weights were optimally chosen—that is, as equal to the inverse of the variance of the measurement error. The precision of the model parameter value estimates was determined from the covariance matrix at the least-squares fit.

Figure 1

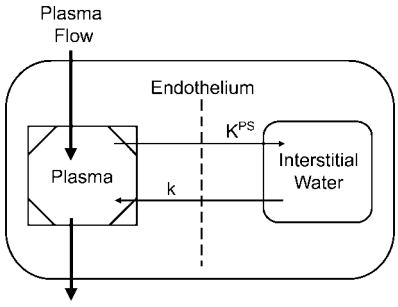

Figure 1: Simple two-compartment tissue model describes kinetics of transport of albumin-$(Gd\text{-}DTPA)_{30}$ from plasma space into interstitial water of tumor. K^{PS} (in microliters per minute per cubic centimeter of tissue) is the endothelial transfer coefficient denoting the clearance of albumin-$(Gd\text{-}DTPA)_{30}$ from plasma to interstitial water. The rate constant k (per minute), which denotes the fractional rate of reflux of albumin-$(Gd\text{-}DTPA)_{30}$ from interstitial water back to plasma, was not resolvable in the time course of the experiment and was therefore set to zero. The box around the plasma compartment denotes a forcing function representing the monoexponetial disappearance of albumin-$(Gd\text{-}DTPA)_{30}$ from the blood. The kinetics of both compartments taken together reflect the dynamic tissue response to albumin-$(Gd\text{-}DTPA)_{30}$ after intravenous bolus administration.

Statistical Analysis

Statistical analysis was performed with software (GraphPad Prism; GraphPad Software, San Diego, Calif). Results are given as mean values ± standard deviations or standard errors of the mean. An unpaired two-tailed Student t test was used to compare the fractional tumor growth rates for the control and the bevacizumab-treated rats. Linear regression analyses were used for correlation of percent K^{PS} change, ΔK^{PS}—calculated as $[(K^{PS}_{day2} - K^{PS}_{day1})/K^{PS}_{day1}] \cdot 100\%$—with fractional tumor growth rate for both the whole tumor and the tumor periphery. Comparison of results of linear regression analysis for whole tumor and tumor periphery was performed according to the technique of Zar (42). One-way analysis of variance was performed to compare K^{PS} values in baseline studies of control and treated animals in both the whole tumor and the tumor periphery. Changes in ΔK^{PS} between control and treated rats for both tumor periphery and whole tumor were also evaluated with one-way analysis of variance. $P < .05$ was considered to indicate a statistically significant difference.

Figure 2

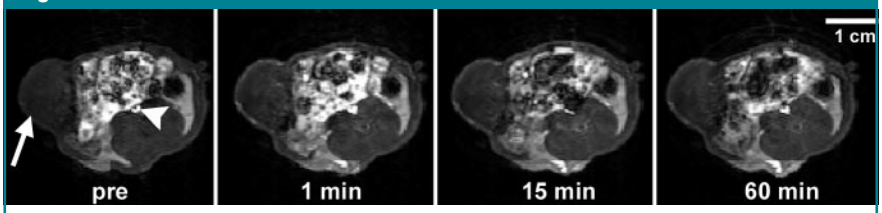

Figure 2: Transverse dynamic T1-weighted MR images obtained in bevacizumab-treated rat after intravenous administration of albumin-$(Gd\text{-}DTPA)_{30}$ at a dose of 0.03 mmol gadolinium per kilogram of body weight show MDA-MB 435 breast cancer (arrow) implanted in mammary zone persistently enhancing for at least 60 minutes, with the strongest tumor enhancement in the rim. Arrowhead = inferior vena cava. *Pre* = before contrast medium administration. (Note the incidental finding of bright signal intensity from the bowel and its contents.) The relatively low but measurable enhancement of the tumor center may reflect the normally high interstitial pressure within the tumor core, which limits local blood flow and transendothelial diffusion of the contrast medium.

Results

Tumor Growth

MDA-MB-435 human breast cancer cells developed into subcutaneous tumors of at least 1.0 cm in diameter within 10–14 days after implantation. Mean tumor volumes at the time of baseline imaging (Fig 2) were measured as 446 mm^3 ± 162 (standard error of the mean) in the control (saline-treated) group ($n = 4$) and as 599 mm^3 ± 73 in the bevacizumab group; this difference was not significant ($P = .27$). However, the fractional rate of tumor growth over the subsequent 11-day treatment and observation period was significantly greater ($P < .05$) in the control (saline-treated) animals (0.224 per day ± 0.066) than in the bevacizumab-treated animals (0.134 per day ± 0.025) (Table 1). This difference was significant ($P < .05$) when all bevacizumab-treated cancers were considered collectively, without regard to specific dose level. When all bevacizumab-treated cancers were considered in this way, tumor growth was significantly retarded, but not completely halted, by bevacizumab treatment (Fig 3).

Quantitative MR Imaging Tumor Characterization

Our simple two-compartment kinetic model of tissue permeability fit the dy-

Acute 24-hour Tumor Responses to Angiogenesis Inhibitory and Saline Treatments

Animal No.	Bevacizumab Dose*	K^{PS} in Tumor Periphery (μL/min/cm³)		K^{PS} in Whole Tumor (μL/min/cm³)		ΔK^{PS} (%)†		Fractional Growth Rate per Day
		Day 1	Day 2	Day 1	Day 2	Tumor Periphery	Whole Tumor	
1	0	17.7	32.5	35.5	38.2	84	8	0.283
2	0	6.5	9.2	6.6	20	42	203	0.266
3	0	11.9	15	15.3	18	26	18	0.212
4	0	33.3	13	26.5	15	−61	−43	0.136
Mean ± standard deviation		17.4 ± 11.6	17.4 ± 10.3	21 ± 12.7	22.8 ± 10.5	23 ± 61	46 ± 108	0.224 ± 0.066
5	0.1	22.9	9.8	9.2	0.2	−57	−98	0.153
6	0.1	27.5	0	22.7	0	−100	−100	0.171
7	0.1	51.1	36.4	55.7	23.2	−29	−58	0.16
Mean ± standard deviation		33.8 ± 15.1	15.4 ± 18.8	29.2 ± 23.9	7.8 ± 13.3	−62 ± 36	−85 ± 23	0.161 ± 0.009
8	0.25	15.8	0	8.4	0	−100	−100	0.112
9	0.25	25.4	0	21.2	12.3	−100	−42	0.149
Mean ± standard deviation		20.6 ± 6.8	0	14.8 ± 9.1	6.2 ± 8.7	−100 ± 0	−71 ± 41	0.131 ± 0.026
10	0.5	17.6	8.4	12.7	14.2	−52	12	0.096
11	0.5	22.4	0	16.5	0	−100	−100	0.141
12	0.5	18.1	0	8.9	0	−100	−100	0.115
13	0.5	100.1	15	84.9	26.3	−85	−69	0.135
14	0.5	69.5	0	58.7	0	−100	−100	0.101
Mean ± standard deviation		45.5 ± 37.5	4.7 ± 6.8	36.3 ± 33.8	8.1 ± 11.9	−87 ± 21	−71 ± 48	0.118 ± 0.02
15	1.0	127.9	17.1	320.2	0	−87	−100	0.167
16	1.0	18.1	0.2	27.1	0	−99	−100	0.11
17	1.0	37.4	0	41.8	0	−100	−100	0.138
Mean ± standard deviation		61.1 ± 58.6	5.8 ± 9.8	129.7 ± 165.1	0	−95 ± 7	−100 ± 0	0.138 ± 0.029

Note.—MR imaging–assayed endothelial transfer coefficients (K^{PS} values) used as a measure of endothelial leakiness of the microvessels in rats with MDA-MB 435 breast cancers before (day 1) and after (day 2) bevacizumab treatment are ordered by increasing dose of angiogenesis inhibitor. Individual fractional tumor growth rates, also tabulated, show significantly more rapid growth in the control (uninhibited) tumors. Fractional tumor growth rate and ΔK^{PS} in control tumors were significantly different from those in bevacizumab-treated tumors ($P < .05$).

* In milligrams per injection.

† Calculated as $[(K^{PS}_{day2} - K^{PS}_{day1})/ K^{PS}_{day1}] \cdot 100\%$.

namic MR imaging data well in all studies, providing acceptable uncertainties for all estimates of K^{PS}, the endothelial transfer coefficient (Fig 4) (mean coefficient of variation, 34 ± 17 [standard deviation]). Strong positive correlations were found between changes in K^{PS} (ΔK^{PS}) in both the whole tumor and the tumor periphery 24 hours after a single administration of either bevacizumab or saline and the fractional tumor growth rate after an 11-day, four-dose course of treatment. As such, the 1-day single-dose percentage K^{PS} change was compatible with its application as a biomarker of tumor growth effects resulting from a prolonged (11-day) multidose treatment. The correlation between percent K^{PS} change and tumor growth rate was significantly stronger ($P < .05$) when the tumor periphery was analyzed (R^2 = 0.74, $P < .001$) than when the whole tumor was selected for analysis (R^2 = 0.45, $P < .05$) (Fig 5). The estimates for K^{PS} at baseline did not differ between control tumors and bevacizumab-treated tumors ($P = .64$) for either the tumor periphery (17.4 μL/min/cm³ ± 11.6 vs 42.6 μL/min/cm³ ± 35.7) or the whole tumor (21.0 μL/min/cm³ ± 12.7 vs 52.9 μL/min/cm³ ± 83.7) (Table). Three of four control animals showed an increase in K^{PS} over 24 hours in both the tumor periphery and the whole tumor, while 13 of 13 bevacizumab-treated animals showed a decrease in K^{PS} in the tumor periphery and the whole tumor (Fig 6). The mean values of these changes in K^{PS} between the control and the bevacizumab-treated groups (with the latter considered as one group) for both tumor periphery (+23% ± 61 vs −85% ± 24) and whole tumor (+46% ± 108 vs −81% ± 34) were significantly different ($P < .05$) (Table).

Discussion

On the basis of our data, the MR imaging–assayed changes in tumor vascular permeability after 1 day of antiangiogenesis treatment correlate positively and significantly with the rate of tumor growth observed at the completion of an extended 11-day course of treatment. These results strongly support the hypothesis that MR imaging–assayed microvessel leakiness of a macromolecular contrast medium may be applied as an early and noninvasive biomarker of tumor responsiveness to angiogenesis-inhibiting drug treatment. Our results go beyond earlier reports that MR imag-

ing–assayed tumor vascular leakiness can be used to monitor the effect of antiangiogenesis drugs (24,29–31) by showing that the MR imaging–measured effect can be detected after only a single dose of the inhibitor and as soon as 24 hours after drug administration. It is specifically this predictive aspect of the MR imaging results that supports the application of results of this dynamic contrast-enhanced MR imaging technique as a biomarker of cancer antiangiogenesis treatment response. Considering the rapid, ongoing development of an enlarging spectrum of cancer angiogenesis-inhibiting drugs designed to attack the angiogenesis process in multiple ways, there is an increasingly strong need for a reliable biomarker. A biomarker able to predict which patient will have a good long-term outcome with a particular treatment regimen could prove to be highly valuable for the individualization of clinical drug choice and dose adjustment.

Figure 3

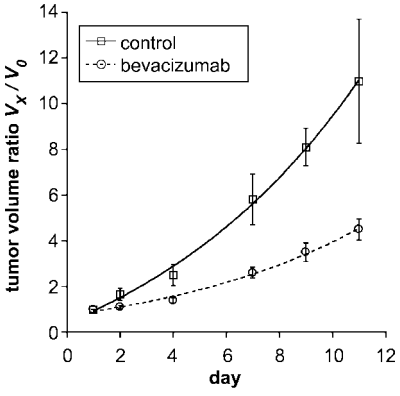

Figure 3: Graph shows tumor volume ratios (tumor volume at day x [V_x] divided by baseline pretreatment tumor volume ([V_0]) given as mean values ± standard errors of the mean (error bars) in control (saline-treated) and bevacizumab-treated tumors over 11 days. Curved lines represent monoexponenial best fits. The tumor volume ratio was significantly higher ($P < .05$) at the completion of tumor treatment (11 days) in the control, uninhibited, saline-treated tumors than in the bevacizumab-treated, angiogenically inhibited tumors.

In our study, the MR imaging permeability (K^{PS}) estimates derived from the 2-mm-wide zone around the periphery of the tumor yielded a better correlation with tumor growth rate (R^2 = 0.74) than the estimates derived from the entire cross-sectional tumor area measurements (R^2 = 0.45), yet results were significant ($P < .05$) with either region of interest. These observations are in agreement with and tend to confirm the conclusions of Preda and colleagues (38), who showed, in a meta-analysis of 98 n-ethyl-n-nitrosourea–induced breast cancers in a rodent model, that the measured permeabilities in the tumor peripheries correlated with histologic tumor grade better than the permeabilities measured for the whole cross-sectional tumor area.

A possible explanation for these observations is that the tumor periphery is located at the interface between neoplastic and non-neoplastic cells and thus is the "front line" of angiogenesis, where vessels from the host tissue sprout and multiply under the influence of tumor-secreted angiogenic factors (43,44). This zone of most active growth and angiogenic activity may thus be the most sensitive location in which to monitor angiogenesis-inhibiting drug therapies.

To achieve the desired graded suppression in vascular permeability (K^{PS}) necessary to demonstrate a potential biomarker relationship with tumor growth and to look for a possible dose-dependent response, we chose to include four dose levels of the anti-VEGF antibody bevacizumab. In general, the higher doses (0.5 and 1.0 mg) of bevacizumab tended to completely suppress vascular permeability to a degree that no further leakage of the macromolecular contrast medium albumin-$(Gd\text{-}DTPA)_{30}$ could be detected with a dynamic MR imaging study. Because of the inclusion of tumors treated with doses of bevacizumab of less than 1.0 mg, a less than complete suppression of permeability was observed that provided the desired graded response that allowed us to better evaluate for a biomarker potential of the MR imaging assay. The robustness of this MR imaging biomarker assay of angiogenesis therapy is supported by the finding that a significant correlation between the 24-hour percent K^{PS} change and the 11-day fractional growth rate suppression was

Figure 4

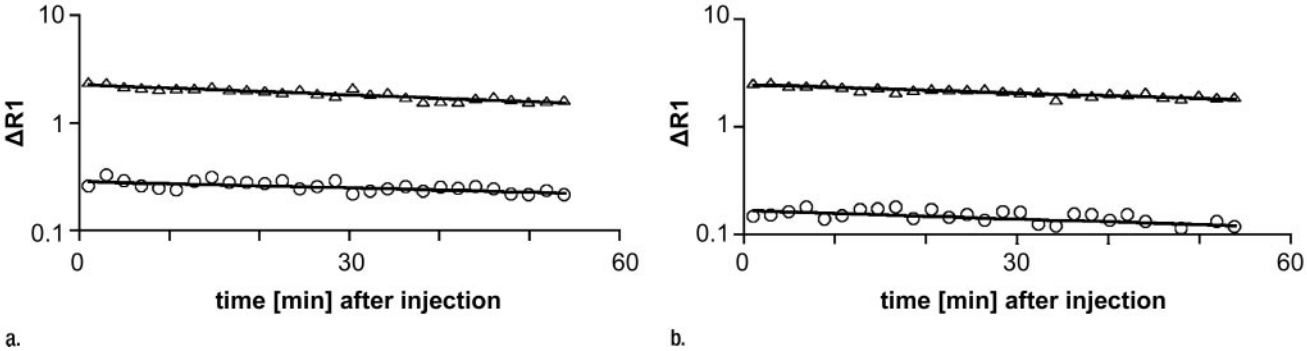

Figure 4: Graphs show representative fits (solid lines) of compartmental model to blood (△) and tumor (○) data after intravenous injection of albumin-$(Gd\text{-}DTPA)_{30}$ **(a)** before and **(b)** 24 hours after bevacizumab administration.

possible, despite the inclusion of many tumors with a nongraded, complete, 100% decline in K^{PS}.

Albumin-(Gd-DTPA)$_{30}$ (34), a 92-kDa derivatized protein, was chosen as the contrast agent for this study because macromolecular contrast agents are especially well suited for the quantitative assay of tumor vascularity, particularly the microvascular permeability to macromolecular solutes. This prototype molecule, which is not intended for human use, has been extensively tested to demonstrate the feasibility and value of macromolecular contrast-enhanced MR imaging for cancer characterization (23,45). As opposed to small molecular solutes less than 1 kDa in weight, macromolecules the size of proteins or larger have been consistently shown to remain intravascular in normal tissues but to pass through the abnormal endothelial barrier into the interstitial extravascular space of virtually all types of cancer—animal and human (9,46,47). Small molecular contrast agents, represented by gadopentetate dimeglumine, with its molecular weight of 938 Da, lack the specificity of macromolecules and diffuse rapidly into the interstitial space of virtually all normal tissues (with the exception of the central nervous system and the testis) and in cancers.

Unfortunately, the leakiness of gadopentetate dimeglumine in cancers is not only rapid but also highly variable; Daldrup et al (40) invasively measured the fraction of gadopentetate dimeglumine that passes from the blood through the vessel wall into the interstitial space on each passage of the blood through the microvascular bed (the so-called extraction fraction) in a human breast cancer model. They reported a range of extraction fraction values from 12% to 45%. Such a broad range for baseline values in cancer vessels would argue against the use of gadopentetate dimeglumine or another relatively small contrast medium for biomarker evaluation of angiogenesis inhibitory therapy. Nonetheless, the use of gadopentetate dimeglumine–enhanced MR imaging results as a biomarker of angiogenesis inhibition should not be dismissed on theoretical grounds: Morgan and colleagues (48) reported a study of liver metastases in advanced colorectal cancers in humans treated with PTK787/ZK222584, a VEGF-receptor tyrosine kinase inhibitor of angiogenesis, in which the dynamic gadopentetate dimeglumine–enhanced MR imaging assays of leakiness, expressed as a bidirectional transfer constant (Ki), correlated

Figure 5

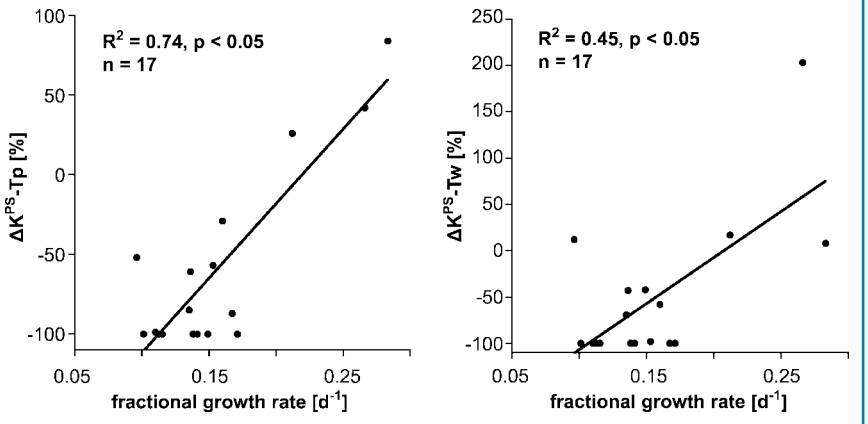

Figure 5: Graphs show correlations between 24-hour changes in MR imaging–assayed vascular leakiness (ΔK^{PS}) after only a single dose of angiogenesis inhibitor or control saline and fractional tumor growth rate at the completion of an 11-day four-dose treatment regimen for **(a)** tumor periphery *(Tp)* and **(b)** whole tumor *(Tw)*. Regardless of whether the leakiness was assayed for the whole tumor or for the tumor periphery, correlations between leakiness and fractional tumor growth rate were statistically significant ($P < .05$). The correlation was notably stronger ($R^2 = 0.74$ vs $R^2 = 0.45$) for the tissue at the tumor periphery, where angiogenesis is presumed to be most active.

Figure 6

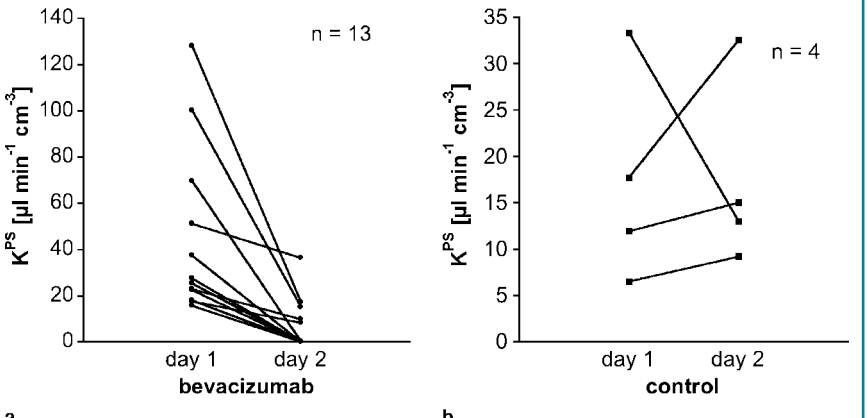

Figure 6: Graphs show individual vascular leakiness (K^{PS}) values at tumor periphery estimated at MR imaging before and 24 hours after a single dose of **(a)** bevacizumab or **(b)** saline. Note that every angiogenically inhibited tumor decreased in estimated microvascular leakiness, while leakiness in three of four control saline-treated tumors and the mean leakiness value for all four saline-treated tumors increased over the same 24-hour period (Table). Apparently the natural trend for control tumors—at least in this human breast cancer model—is for increasing microvascular leakiness with increasing tumor age and growth. In theory, this could be a reflection of increasing VEGF production by the growing mass of tumor cells.

significantly but relatively weakly with the 56-day growth suppression of liver metastases ($R^2 = 0.37$, $P < .05$).

Our decision to use a macromolecular contrast agent for this biomarker study was consistent with the observations of Roberts et al (49), who reported that the errors inherent to MR imaging assays of microvascular characteristics are magnified with small-molecular contrast agents as compared with macromolecular albumin-(Gd-DTPA)$_{30}$, which has a prolonged intravascular half-life of 2 hours and a volume of distribution, 0.05 L/kg, that matches the plasma volume of the rat body.

Our study and the possible translation of its results to clinical practice were limited in several ways. Only a single duration of treatment, 11 days, was used to estimate the long-term effect of bevacizumab on tumor growth. Unfortunately, a longer course of angiogenesis inhibition would not have been feasible because the saline-treated, uninhibited control tumors would have grown excessively and caused unacceptable morbidity. The chosen contrast medium, albumin-(Gd-DTPA)$_{30}$, is a prototype macromolecular agent that is not intended for development as a clinical drug. But other macromolecular formulations, such as ultrasmall superparamagnetic iron oxide particles, now awaiting governmental approval in the United States for clinical use would be expected to distribute in cancers much like albumin-(Gd-DTPA)$_{30}$ (45) and thus might allow a feasible translation of this method to clinical practice in the near future.

In conclusion, the correlation between the change in tumor vessel leakiness assayed with MR imaging in the tumor periphery induced by a single dose of bevacizumab and the observed change in tumor growth after a prolonged, multidose course of bevacizumab was strong ($R^2 = 0.74$).

Practical application: Our results suggest that an MR imaging assay such as we used might be useful for the care and treatment of patients with cancer who are being considered for angiogenesis-inhibiting drug treatment. At the onset of therapy, the MR imaging assay of tumor vessel permeability could be applied to predict which patients should be expected to have a good long-term drug response, while patients with a poor or absent response on the MR imaging permeability assay might be considered for a different drug regimen or a different dose of inhibitor. Our initial results in experimental animals may encourage the further development for clinical use of MR imaging macromolecular contrast media and their specific application for quantitative, noninvasive evaluation of tumor microvessel permeability. MR imaging biomarkers predictive of tumor response to angiogenesis inhibitors could be of substantial clinical value and find widespread clinical application.

References

1. Brown LF, Berse B, Jackman RW, et al. Expression of vascular permeability factor (vascular endothelial growth factor) and its receptors in breast cancer. Hum Pathol 1995; 26:86–91.
2. Couvelard A, Paraf F, Gratio V, et al. Angiogenesis in the neoplastic sequence of Barrett's oesophagus: correlation with VEGF expression. J Pathol 2000;192:14–18.
3. Dobbs SP, Brown LJ, Ireland D, et al. Platelet-derived endothelial cell growth factor expression and angiogenesis in cervical intraepithelial neoplasia and squamous cell carcinoma of the cervix. Ann Diagn Pathol 2000; 4:286–292.
4. Dobbs SP, Hewett PW, Johnson IR, Carmichael J, Murray JC. Angiogenesis is associated with vascular endothelial growth factor expression in cervical intraepithelial neoplasia. Br J Cancer 1997;76:1410–1415.
5. Magennis DP. Angiogenesis: a new prognostic marker for breast cancer. Br J Biomed Sci 1998;55:214–220.
6. Weidner N, Folkman J. Tumoral vascularity as a prognostic factor in cancer. Important Adv Oncol 1996;:167–190.
7. Folkman J. Tumor angiogenesis: therapeutic implications. N Engl J Med 1971;285:1182–1186.
8. Vermeulen PB, Gasparini G, Fox SB, et al. Second international consensus on the methodology and criteria of evaluation of angiogenesis quantification in solid human tumours. Eur J Cancer 2002;38:1564–1579.
9. Jain RK. Transvascular and interstitial transport in tumors. Adv Exp Med Biol 1988;242: 215–220.
10. Jain RK. Tumor angiogenesis and accessibility: role of vascular endothelial growth factor. Semin Oncol 2002;29:3–9.
11. Folkman J, Ingber D. Inhibition of angiogenesis. Semin Cancer Biol 1992;3:89–96.
12. Inai T, Mancuso M, Hashizume H, et al. Inhibition of vascular endothelial growth factor (VEGF) signaling in cancer causes loss of endothelial fenestrations, regression of tumor vessels, and appearance of basement membrane ghosts. Am J Pathol 2004;165: 35–52.
13. McDonald DM, Choyke PL. Imaging of angiogenesis: from microscope to clinic. Nat Med 2003;9:713–725.
14. Hashizume H, Baluk P, Morikawa S, et al. Openings between defective endothelial cells explain tumor vessel leakiness. Am J Pathol 2000;156:1363–1380.
15. Schwickert HC, Stiskal M, Roberts TP, et al. Contrast-enhanced MR imaging assessment of tumor capillary permeability: effect of irradiation on delivery of chemotherapy. Radiology 1996;198:893–898.
16. Preda A, Novikov V, Moglich M, et al. Magnetic resonance characterization of tumor microvessels in experimental breast tumors using a slow clearance blood pool contrast agent (carboxymethyldextran-A2-Gd-DOTA) with histopathological correlation. Eur Radiol 2005; 15:2268–2275.
17. Brasch R, Pham C, Shames D, et al. Assessing tumor angiogenesis using macromolecular MR imaging contrast media. J Magn Reson Imaging 1997;7:68–74.
18. Dvorak HF, Nagy JA, Feng D, Brown LF, Dvorak AM. Vascular permeability factor/vascular endothelial growth factor and the significance of microvascular hyperpermeability in angiogenesis. Curr Top Microbiol Immunol 1999;237:97–132.
19. Dvorak HF, Brown LF, Detmar M, Dvorak AM. Vascular permeability factor/vascular endothelial growth factor, microvascular hyperpermeability, and angiogenesis. Am J Pathol 1995;146:1029–1039.
20. Jain RK. Transport of molecules across tumor vasculature. Cancer Metastasis Rev 1987;6:559–593.
21. Jain RK, Gerlowski LE. Extravascular transport in normal and tumor tissues. Crit Rev Oncol Hematol 1986;5:115–170.
22. Gossmann A, Okuhata Y, Shames DM, et al. Prostate cancer tumor grade differentiation with dynamic contrast-enhanced MR imaging in the rat: comparison of macromolecu-

lar and small-molecular contrast media—preliminary experience. Radiology 1999; 213:265–272.

23. Brasch RC, Shames DM, Cohen FM, et al. Quantification of capillary permeability to macromolecular magnetic resonance imaging contrast media in experimental mammary adenocarcinomas. Invest Radiol 1994; 29(suppl 2):S8–S11.

24. Gossmann A, Helbich TH, Mesiano S, et al. Magnetic resonance imaging in an experimental model of human ovarian cancer demonstrating altered microvascular permeability after inhibition of vascular endothelial growth factor. Am J Obstet Gynecol 2000; 183:956–963.

25. Turetschek K, Roberts TP, Floyd E, et al. Tumor microvascular characterization using ultrasmall superparamagnetic iron oxide particles (USPIO) in an experimental breast cancer model. J Magn Reson Imaging 2001; 13:882–888.

26. Daldrup-Link HE, Rydland J, Helbich TH, et al. Quantification of breast tumor microvascular permeability with feruglose-enhanced MR imaging: initial phase II multicenter trial. Radiology 2003;229:885–892.

27. Daldrup H, Shames DM, Wendland M, et al. Correlation of dynamic contrast-enhanced MR imaging with histologic tumor grade: comparison of macromolecular and small-molecular contrast media. AJR Am J Roentgenol 1998;171:941–949.

28. Turetschek K, Preda A, Floyd E, et al. MRI monitoring of tumor response following angiogenesis inhibition in an experimental human breast cancer model. Eur J Nucl Med Mol Imaging 2003;30:448–455.

29. Preda A, Novikov V, Moglich M, et al. MRI monitoring of Avastin antiangiogenesis therapy using B22956/1, a new blood pool contrast agent, in an experimental model of human cancer. J Magn Reson Imaging 2004;20: 865–873.

30. Turetschek K, Preda A, Floyd E, et al. MRI monitoring of tumor response to a novel VEGF tyrosine kinase inhibitor in an experimental breast cancer model. Acad Radiol 2002;9(suppl 2):S519–S520.

31. Wiart M, Fournier LS, Novikov VY, et al. Magnetic resonance imaging detects early changes in microvascular permeability in xenograft tumors after treatment with the matrix metalloprotease inhibitor Prinomastat. Technol Cancer Res Treat 2004;3:377–382.

32. Pham CD, Roberts TP, van Bruggen N, et al. Magnetic resonance imaging detects suppression of tumor vascular permeability after administration of antibody to vascular endothelial growth factor. Cancer Invest 1998;16:225–230.

33. Cailleau R, Olive M, Cruciger QV. Long-term human breast carcinoma cell lines of metastatic origin: preliminary characterization. In Vitro 1978;14:911–915.

34. Ogan MD, Schmiedl U, Moseley ME, Grodd W, Paajanen H, Brasch RC. Albumin labeled with Gd-DTPA: an intravascular contrast-enhancing agent for magnetic resonance blood pool imaging—preparation and characterization. Invest Radiol 1987;22:665–671.

35. Olszewski AJ, Grossbard ML, Kozuch PS. The horizon of antiangiogenic therapy for colorectal cancer. Oncology (Williston Park) 2005;19:297–306.

36. Midgley R, Kerr D. Bevacizumab: current status and future directions. Ann Oncol 2005;16:999–1004.

37. Shames DM, Kuwatsuru R, Vexler V, Muhler A, Brasch RC. Measurement of capillary permeability to macromolecules by dynamic magnetic resonance imaging: a quantitative noninvasive technique. Magn Reson Med 1993;29:616–622.

38. Preda A, Turetschek K, Daldrup H, et al. The choice of region of interest measures in contrast-enhanced magnetic resonance image characterization of experimental breast tumors. Invest Radiol 2005;40:349–354.

39. Roberts TP, Brasch RC, Schwickert HC, et al. Quantification of tissue gadolinium concentration using magnetic resonance imaging: comparison of ultrashort inversion time inversion recovery echoplanar and dynamic three-dimensional spoiled gradient-recalled approaches with in vitro measurements. Acad Radiol 1996;3(suppl 2):S282–S285.

40. Daldrup HE, Shames DM, Husseini W, Wendland MF, Okuhata Y, Brasch RC. Quantification of the extraction fraction for gadopentetate across breast cancer capillaries. Magn Reson Med 1998;40:537–543.

41. Foster DM, Boston RC, Jacquez JA, Zech L. A resource facility for kinetic analysis: modeling using the SAAM computer programs. Health Phys 1989;57(suppl 1):457–466.

42. Zar JH. Biostatistical analysis. 4th ed. Englewood Cliffs, NJ: Prentice-Hall, 1999.

43. Koukourakis MI, Giatromanolaki A, Sivridis E, Fezoulidis I. Cancer vascularization: implications in radiotherapy? Int J Radiat Oncol Biol Phys 2000;48:545–553.

44. Matsubayashi R, Matsuo Y, Edakuni G, Satoh T, Tokunaga O, Kudo S. Breast masses with peripheral rim enhancement on dynamic contrast-enhanced MR images: correlation of MR findings with histologic features and expression of growth factors. Radiology 2000;217:841–848.

45. Turetschek K, Huber S, Helbich T, et al. Dynamic MRI enhanced with albumin-(Gd-DTPA)30 or ultrasmall superparamagnetic iron oxide particles (NC100150 injection) for the measurement of microvessel permeability in experimental breast tumors. Acad Radiol 2002;9(suppl 1):S112–S114.

46. Gerlowski LE, Jain RK. Microvascular permeability of normal and neoplastic tissues. Microvasc Res 1986;31:288–305.

47. Dvorak HF, Nagy JA, Dvorak JT, Dvorak AM. Identification and characterization of the blood vessels of solid tumors that are leaky to circulating macromolecules. Am J Pathol 1988;133:95–109.

48. Morgan B, Thomas AL, Drevs J, et al. Dynamic contrast-enhanced magnetic resonance imaging as a biomarker for the pharmacological response of PTK787/ZK 222584, an inhibitor of the vascular endothelial growth factor receptor tyrosine kinases, in patients with advanced colorectal cancer and liver metastases: results from two phase I studies. J Clin Oncol 2003;21:3955–3964.

49. Roberts TP, Helbich TH, Ley S, et al. Utility (or not) of Gd-DTPA-based dynamic MRI for breast cancer diagnosis and grading. Acad Radiol 2002;9(suppl 1):S261–S265.